energy&fuels

Article

pubs.acs.org/EF

Mechanism for Inhibition of Atmospheric-Pressure Syngas/Air Flames by Trimethylphosphate

Vladimir M. Shvartsberg,* Andrey G. Shmakov, Tatyana A. Bolshova, and Oleg P. Korobeinichev

Institute of Chemical Kinetics and Combustion, Novosibirsk 630090, Russia

ABSTRACT: The effect of the addition of trimethylphosphate on the propagation of atmospheric-pressure syngas/air flames of different stoichiometry was investigated experimentally and numerically. The inhibition effectiveness determined from experimental observations was shown to have a minimum at the equivalence ratio of 1.5 and to increase substantially with an increasing equivalence ratio. The modeling did not predict the minimum of the inhibition effectiveness but satisfactorily predicted its increase with an increase of the equivalence ratio. Sensitivity analysis showed that the effectiveness rise correlated with the relative increase in the net rate of the reaction CO + OH = CO_2 + H, which is known to be the main pathway for CO oxidation. The decrease in the net reaction rate was explained by a reduction in the OH mole fraction as the inhibitor was added to the flames. The reduction in the OH concentration is not due to OH recombination in reactions involving phosphorus but is due to a decrease in its production rate in syngas oxidation reactions because of the removal of H atoms from the flames via their recombination catalyzed by phosphorus-containing species.

1. INTRODUCTION

Synthetic gas mixtures, better known as syngas, are traditionally used in the chemical industry to produce methanol and some other products of organic synthesis, including Fischer−Tropsch synthesis of paraffins. Hydrogen/carbon monoxide oxidation kinetics is of great interest in combustion research over many years, because it forms an important building block of the hydrocarbon combustion chemistry. Recently, there has been increased interest in the combustion of syngas because of its use as an alternative environmentally safe fuel for gas turbines. At the moment, the power generation is one of the most promising research areas with the development and optimization of integrated gasification combined cycle plants. Gasification processes allow for a wide range of solid combustibles, including coal, biomass, and municipal solid wastes, to be converted into syngas mixtures that can be burned in gas turbines to generate electricity. In the near future, the efficiency of coal gasification is expected to be increased to a level at which syngas will be able to compete with natural gas. The prospects of using alternative fuels, including syngas, are associated with a reduction in atmospheric pollution and fuel production from biomass, plant raw material, and organic wastes.

Combustion of syngas/air mixtures has been extensively studied both experimentally and by modeling.[1−15] At present, a number of reaction mechanisms for syngas oxidation have been developed.[3−10,12,15] Some of them are out of date, but the latest ones[10,12,15] satisfactorily predict flame speeds over a wide range of equivalence ratios at atmospheric and elevated pressures and elevated initial temperatures.

An expanding large-scale production of syngas mixtures and their application as a fuel for gas turbines has put in the forefront the problem of fire safety. It is so important because carbon monoxide/hydrogen mixtures are more flammable than natural gas and other hydrocarbons. According to Wierzba and Kilchyk,[16] mixtures of air with carbon monoxide containing a minimal admixture of water are flammable at the CO volume fraction from about 0.135 to 0.675 under normal conditions. Flammability limits of syngas/air mixtures with a high content of hydrogen are very close to those of pure hydrogen.[16] Inhibition by chemically active compounds is known to be one of the most available and convenient methods for reducing the flammability of a fuel. Therefore, a study of inhibition chemistry of syngas flames is an important object of current interest.

Inhibition of syngas flames has been studied insufficiently. Safieh et al.[17] investigated the effect of CF_3Br on the structure of a burner-stabilized $CO/H_2/O_2/Ar$ flame at 50 Torr. Measured concentration profiles of stable and labile flame species suggest the presence of two flame zones. In the first zone, adjacent to the preheating zone of the flame, H and OH radicals interact with the inhibitor and its combustion products. In the second zone, CO oxidation occurs.

Vandooren et al.[18] used molecular beam mass spectrometry to study the inhibition of $CO/H_2/O_2/Ar$ flame by CF_3H. Combustion products of the inhibitor responsible for the removal of OH radicals from the flame were identified. It has been shown[18] that hydrogen formation in the reaction CF_3H + H = CF_3 + H_2 is slower than HBr formation in a flame doped with CF_3Br.[16] This is one of the reasons for the low inhibition effectiveness of CF_3H. Later, Linteris[19] improved the model for flame inhibition by CF_3H.

Chang et al.[20] elaborated a model for the inhibition of CO flames by chlorine. There is some disagreement between the modeling results and experimental data. One of the most interesting observations is as follows: At a low Cl/H ratio in the flame, inhibition is due to H-atom recombination catalyzed by HCl. At a high Cl/H ratio, the catalytic recombination of H and OH dominates and controls the flame speed.

Received: June 19, 2012
Revised: August 9, 2012
Published: August 10, 2012

 © 2012 American Chemical Society dx.doi.org/10.1021/ef301036p | *Energy Fuels* 2012, 26, 5528−5536

Rumminger and Linteris[21] made a substantial contribution to understanding the mechanism for inhibition of premixed $CO/H_2/O_2/N_2$ flames by iron pentacarbonyl, $Fe(CO)_5$. The authors measured and simulated the burning velocity of the flames with and without the inhibitor over a range of initial H_2 and O_2 mole fractions. The experimental and modeling results obtained are in good agreement, especially for the uninhibited flames. The agreement strongly depends upon the rate of the $CO + OH = CO_2 + H$ reaction and the rates of several key iron-involving reactions in catalytic H- and O-atom recombination cycles. It was found that the O-atom cycle not being important in methane flames plays a crucial role in syngas flames. The H-atom cycle that causes most of the radical scavenging in the methane flames is also active in $CO-H_2$ flames but is of secondary importance.

The goal of studies of flame inhibition by chemically active additives is not only to investigate the effect of an inhibitor on combustion or self-ignition but also to elucidate the mechanism of fuel combustion under particular conditions and understand the role of and interplay between various processes in flames that are difficult to observe without inhibitors. The objective of the present study was to investigate the effect of the catalytic recombination of H, O, and OH on the speed of atmospheric-pressure syngas/air flames and the rates of key reactions of syngas oxidation. In addition, in this work, we plan to study the influence of the equivalence ratio on catalytic recombination reactions and other processes in the flame.

2. EXPERIMENTAL AND MODELING APPROACHES

2.1. Measurements of Flame Speed. We studied a mixture of syngas (CO/H_2 = 95:5) with air at a initial temperature of 298 ± 2 K and atmospheric pressure. The choice of the $CO + H_2$ mixture with low H_2 content for our research is motivated by our interest in the action of phosphorus-containing inhibitor on the combustion chemistry of carbon monoxide. In the meantime, the combustion chemistry of the syngas mixture with a high H_2 concentration is determined largely by hydrogen oxidation. On the other hand, combustion of CO with a minor admixture of H_2 is promoted by trimethylphosphate (TMP) because of H atoms in its molecules. Therefore, we have selected a syngas composition in which burning velocity has low sensitivity to H_2 addition. Burning velocity was measured using a Mache–Hebra nozzle burner[22] and the total area method[23] from flame images, as was performed by Linteris and Truett.[24] The burner consisted of a 27 cm quartz tube with an area contraction ratio of 4.7 (over a 3 cm length) and a nozzle exit with an inner diameter of 0.9 cm. The contraction ratio is a ratio of section areas of the tube to the outer nozzle of the burner. The nozzle contour was designed to obtain a straight-sided visible image of the flame cone. The burning velocity was measured using digitized images of cones in shadow photographs taken with a charge-coupled device (CCD) camera (Figure 1). Actual resolution of the CCD camera was 3648 × 2746 = 9.55 megapixels.

Gas flows were measured with a mass flow controller (MKS Instruments, model 1299S) calibrated with a wet gas meter with an accuracy of ±1%. The volumetric flow rate of the combustible mixture was varied from 0.9 to 6.6 standard liters per minute (slpm). TMP (Merck, purity > 98%) was added to the combustible mixture (300 ± 25 ppm) using a saturator with liquid TMP in a controlled temperature bath (22 ± 1 °C).

The estimated confidence interval for the burning velocity was ±6–8%. In estimating the accuracy of our speed measurements, we took into account, first, the error in measuring the volumetric flow rate of unburnt gases (up to ±0.6%) and, second, the error in measuring the surface of the flame cone (±5%). The maximum error in measuring the equivalence ratio was ±1.4%, but its influence on the flame speed falls within the limits of the confidence interval.

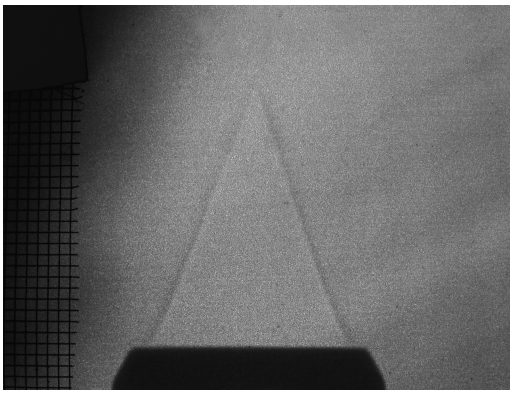

Figure 1. Digitized image of the flame cone in shadow photographs taken with a CCD camera.

Measured flame speeds were compared to literature data[12−14,25] (Figure 2). The maximum difference of about 8% between our results and those reported by McLean et al., Hassan et al., and Sun et al.[12−14] is observed for rich flames.

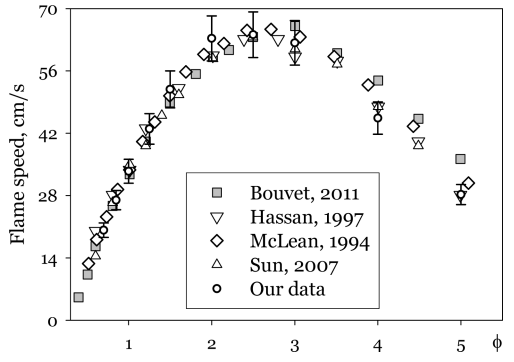

Figure 2. Measured and literature data of the speed of syngas/air flames without additives versus the equivalence ratio.

2.2. Modeling. The speed and structure of syngas/air flames doped with TMP at a pressure of 1 bar were simulated using mechanisms for syngas oxidation[12] and flame inhibition by TMP.[26] Spatial variations in the rates of production of chain carriers via reactions involving phosphorus-containing species (PCS) and net reaction rates in the flames were calculated using the KINALC code,[27] a postprocessor of the output files of the PREMIX code.[28,29] Because the reaction mechanism used in the calculations contained only reversible reactions, the original mechanisms[12,25] were first rendered irreversible using the MECHMOD code.[30] We note that, although the production rate via particular reactions was calculated by irreversible reactions, below it is given as a net reaction rate for the reversible reaction.

Windward differencing was used, and the grid was refined to GRAD = 0.1 and CURV < 0.2 (parameters controlling the number of grid points inserted in regions of high gradient and high curvature in the PREMIX code). These values of GRAD and CURV provided a sufficient refinement of the grid, so that the resulting flame speed was independent of the number of grid points (≈200–250 required). In all calculations, the energy equation was solved and multicomponent and thermal diffusions were used.

3. RESULTS AND DISCUSSION

3.1. Effect of TMP on the Flame Speed. Figure 3 shows measured and simulated speeds of syngas/air flames doped with 0.03% TMP versus the equivalence ratio. The experimental and modeling data for the undoped flames are generally in satisfactory agreement, although for rich flames with ϕ = 4

dx.doi.org/10.1021/ef301036p | Energy Fuels 2012, 26, 5528–5536

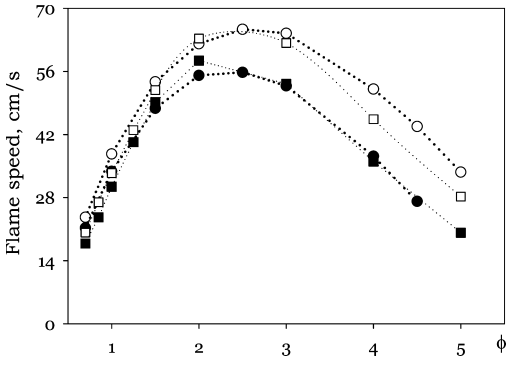

Figure 3. Measured (□ and ■) and simulated (○ and ●) speeds of syngas/air flames without additives (□ and ○) and doped with 0.03% TMP (■ and ●) versus the equivalence ratio.

and 5, the discrepancy exceeds the declared error of 8% (14 and 16%, respectively).

In the case of TMP-doped flames, there is remarkable accordance between modeling and experimental results, which is much better than that for methane flames.[31] We had difficulty explaining the better agreement between the experiment and modeling for the doped flames. It may be mentioned that the combustion chemistry of syngas-rich flames is simpler compared to hydrocarbons, in which soot precursors are not formed. The interaction of phosphorus-containing compounds with soot precursors has not been studied and is not considered in the mechanism.[26]

Figure 4 shows the inhibition effectiveness derived from experimental and modeling data and expressed as $E = (u_0 - u)/$

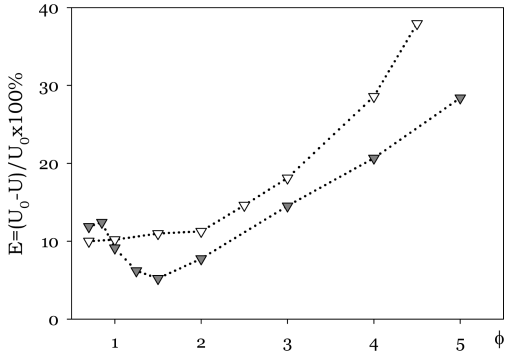

Figure 4. Inhibition effectiveness expressed as a relative decrease in flame speed with the addition of TMP versus the equivalence ratio, determined from experimental (gray ▼) and modeling (▽) data.

$u_0 \times 100\%$ (u_0 is the undoped flame speed, and u is the speed of the TMP-doped flame) versus the equivalence ratio. The experimental curve of the inhibition effectiveness versus ϕ has a minimum at $\phi = 1.5$ ($E \approx 5\%$); for the leanest flame, the measured effectiveness is 11%, and for the richest flames, the measured effectiveness is 28%. Modeling predicts a monotonic increase in the effectiveness with an increasing equivalence ratio. In the range of ϕ from 0.7 to 1.5, the effectiveness changes insignificantly, but at $\phi = 2$ and more, it grows rapidly and reaches 41% at $\phi = 4.5$. It is noteworthy that, at a TMP concentration of 0.03% by volume, the inhibition effectiveness, especially in flames with $\phi = 4$ and 4.5, is much higher than that in hydrocarbon flames. It is interesting to note that inhibition of $CO/H_2/O_2/N_2$ flames by iron pentacarbonyl[21] is less effective than for hydrocarbon flames. It may be explained by the key role of O-atom catalytic recombination in these flames, whereas the H-atom scavenging cycle plays a crucial role in methane flames.[21] The concentration of the O atom in near-stoichiometric and rich flames is lower than that of the H atom; therefore, the rate of O-atom scavenging is not so high as H-atom catalytic recombination in methane flames.

It is well-known that flame inhibition by PCS and other chemically active inhibitors involves the removal of active chain carriers from the flame via catalytic recombination reactions. To understand the factors responsible for differences in inhibition effectiveness for flames at different equivalence ratios, we compared and quantitatively evaluated the inhibitor effect on active flame species by integrating the rate-of-production profiles with respect to the distance transverse to the flame front. This approach was proposed and successfully applied earlier.[32] The integration region coincided with the flame reaction zone, i.e., from the unburnt gases to flame cross-section with maximum H and OH levels (actually from −0.01 to about 0.05 cm for all flames). Figure 11 shows that, at 0.5 cm, the net rate PCS-involving reactions is close to 0.

3.2. Mechanism for Syngas/Air Flame Inhibition by TMP. Speaking about a mechanism for flame inhibition, we mean, on the one hand, reactions involving inhibitor-related species in which the chain carriers are removed from the flame and, on the other hand, chemical processes controlling the inhibition effectiveness (E) variation versus the equivalence ratio.

Figure 5 gives integrals of the production rate of H, O, and OH in PCS-involving reactions versus the equivalence ratio for

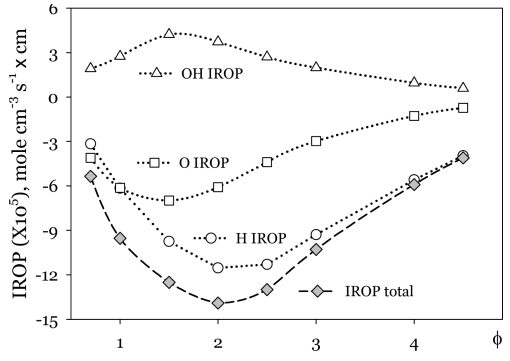

Figure 5. IROPs of H, O, and OH and the total IROP of these species in reactions involving PCS in syngas/air flames doped with 0.03% TMP versus the equivalence ratio.

TMP-doped flames. The results clearly show that TMP-derived species catalyze the removal of H and O atoms from the flames and generate OH radicals. The extreme point for the H curve is observed at $\phi \approx 2$, and those for O and OH are observed at $\phi = 1.5$. The integrated production rates (IROPs) of O and OH are similar in magnitude but opposite in sign, especially at $\phi = 2.5$–4.5. The total IROP of H, O, and OH differs only slightly from the production rate of atomic H. Hence, the action of TMP as an inhibitor is essentially realized in the removal of H atoms from the flames, as shown earlier.[26]

Furthermore, the additive provides an additional channel for OH production. This is an unexpected result because it has previously been believed that phosphorus compounds mainly catalyze H and OH recombination. It is now clear that this occurs not in all flames. Of course, H and OH recombination proceeds in some reactions, but the integral of the net rate of

dx.doi.org/10.1021/ef301036p | Energy Fuels 2012, 26, 5528–5536

OH production is positive in all studied TMP-doped flames. Hereupon, it would be interesting to calculate the rate of production of active species in TMP-doped hydrocarbon and hydrogen flames to understand the recombination processes of the active species catalyzed by PCS. It is interesting to note that the curves shown in Figure 5 have the same shape as similar data for H_2/air flames doped with atomic iron.[32]

Data in Figure 5 show the inhibition chemistry of syngas flames by the TMP additive to change with the equivalence ratio variation. It should be read as a change of ratios of the net rate of the PCS-involving reactions and their contribution into the total rate of H- and O-atom consumption. The production of OH via PCS-involving reactions will be shown below to make a minor contribution to the inhibition effectiveness, and therefore, the pathways of OH production are not analyzed in this research.

Figure 6 shows the spatial variation of the net rate of production of H atoms via the key PCS-involving steps along the zone of flames with ϕ = 0.7, 2, and 4.5. It is noteworthy that we compared the rates of production of H and O via all PCS-involving reactions, but the production rate via the reactions, which are not given in the figure, are too small to be shown graphically. The crucial PCS-involving reactions substantially contributing to the total consumption rate of H atoms are given below.

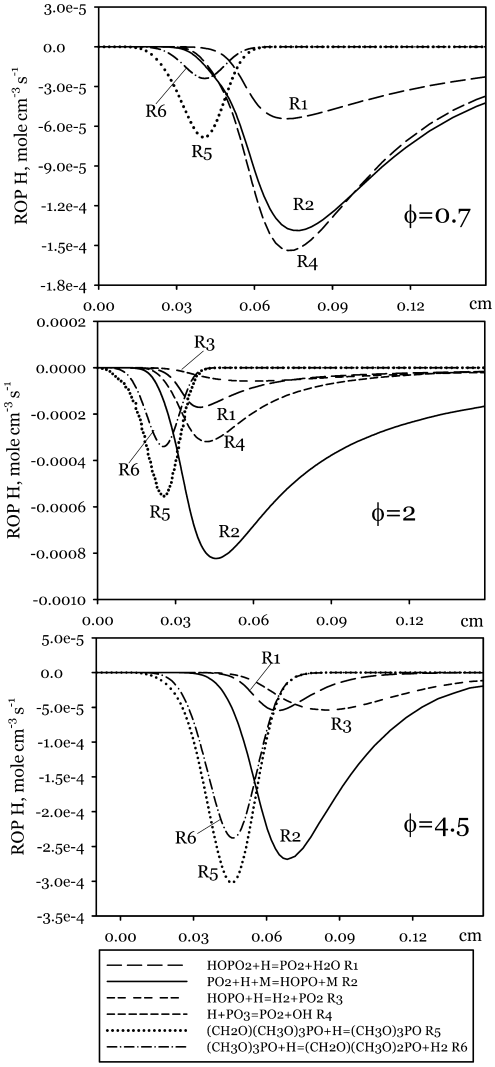

Figure 6. Spatial variation of the rate of production of H atoms via crucial PCS-involving reactions in TMP-doped flames with ϕ = 0.7, 2, and 4.5.

$$HOPO_2 + H = PO_2 + H_2O \quad (R1)$$

$$PO_2 + H + M = HOPO + M \quad (R2)$$

$$HOPO + H = H_2 + PO_2 \quad (R3)$$

$$H + PO_3 = PO_2 + OH \quad (R4)$$

$$(CH_3O)_3PO + H = (\bullet CH_2O)(CH_3O)_2PO + H_2 \quad (R5)$$

$$(\bullet CH_2O)(CH_3O)_2PO + H = (CH_3O)_3PO \quad (R6)$$

The analysis of Figure 6 allowed us to make the following conclusions: (1) The consumption rate of H atoms via reaction R1 does not differ in the flames with ϕ = 0.7 and 4.5. The consumption rate of H atoms via reaction R1 in the flame with ϕ = 2 is about 3.5 times higher than what is explained by a higher concentration of hydrogen atoms in this flame. (2) Reaction R2 makes the maximal contribution to the consumption rate of H atoms in practically all flames, and only in the lean flame, the contribution of R3 is a little bit less. The high net rate of reaction R3 in the lean flame (in the stoichiometric flame, its net rate is already less than that of reaction R2) is explained by the excess of O_2 and, therefore, high concentration of PO_3 that quickly reduces in the rich flames. The leading role of reaction R2 in scavenging of H atoms in practically all studied flames may be explained by a relatively high PO_2 level in the flames cross-section, where the H concentration is maximal. PO_2 in this cross-section comprises from 11 to 48% of the flame phosphorus depending upon the equivalence ratio. (3) As the equivalence ratio rises, the contribution of reactions R5 and R6 involving organophosphates TMP and $(\bullet CH_2O)(CH_3O)_2PO$ to the rate of H consumption increases. The increase in the contribution of the reactions R5 and R6 especially in the richest flame occurs because of a decrease in the H consumption rate via reactions R1−R4 rather than an increase in reaction R5 and R6 net rates. The low net rate of reactions R1 and R4 in the flame with ϕ = 4.5 is quite clear. It is explained by a low concentration of PCS with a high oxidation number including PO_3 and $HOPO_2$ in the rich flame. A low rate of H consumption via reaction R2 in the flame with ϕ = 4.5 in comparison to that with ϕ = 2 is explained by the lower concentration of the reagents: 2 time decrease in the H level and 4 time decrease in the PO_2 level. At a first glance, a low rate of consumption of H atoms via reaction R3 in the richest flame is not quite clear because HOPO is the basic PCS in the flame. A lower (for about 500 K) temperature of the flame with ϕ = 4.5 in comparison to that with ϕ = 2 can also not explain such a low net rate of reaction R3. As is evident, under these conditions, the rate of the reverse reaction is rather high.

Thus, the total rate of production of H atoms via PCS-involving reactions is basically determined by the reagents level rather than the flame temperature. Therefore, the nature of the variation of the integrated rates of production of the chain carriers (Figure 5) becomes clear. The concentration of H atoms is minimal in the lean flame (ϕ = 0.7) and increases, reaching its maximum at ϕ = 2−3, growing in about 6 times. A further increase in the equivalence ratio up to 4.5 led to a fall of the H level in about 2 times. The composition of PCS in the

dx.doi.org/10.1021/ef301036p | Energy Fuels 2012, 26, 5528−5536

reaction zone of the flame obviously influences the rate of H-atom production.

Figure 7 shows the spatial variation of the net rate of production of O atoms via the crucial PCS-involving reactions

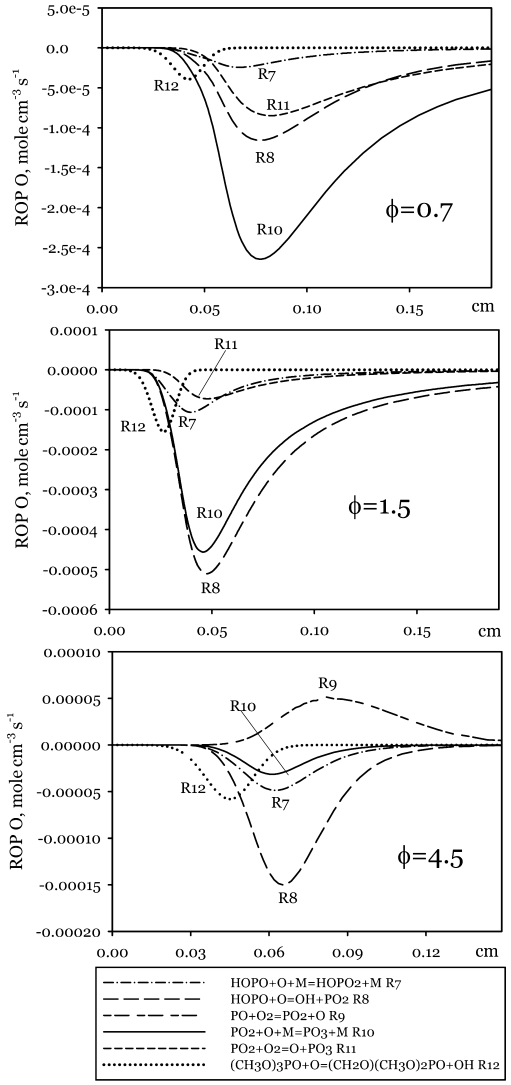

Figure 7. Spatial variation of the rate of production of O atoms via crucial PCS-involving reactions in TMP-doped flames with ϕ = 0.7, 1.5, and 4.5.

along the zone of flames with ϕ = 0.7, 2, and 4.5. The crucial PCS-involving reactions substantially contributing to the total consumption rate of H atoms are given below.

$$HOPO + O + M = HOPO_2 + M \quad (R7)$$

$$HOPO + O = PO_2 + OH \quad (R8)$$

$$PO + O_2 = PO_2 + O \quad (R9)$$

$$PO_2 + O + M = PO_3 + M \quad (R10)$$

$$PO_2 + O_2 = PO_3 + O \quad (R11)$$

$$(CH_3O)_3PO + O = (\bullet CH_2O)(CH_3O)_2PO + OH \quad (R12)$$

The data shown in Figure 7 obviously demonstrate that, in the lean flame (ϕ = 0.7), reaction R10 plays a crucial role in removing O atoms. A high consumption rate of O atoms via reaction R10 can be explained by a relatively high concentration of PO_2 (in comparison to HOPO) in the lean flame. The consumption rate of O atoms via reaction R8 is about 2.5 times lower because of a low HOPO level in lean flames. In the flame with ϕ = 1.5, where the O level reaches it maximum and the HOPO concentration is noticeably higher than in the lean flame, reactions R8 and R10 make main contributions to O-atom consumption.

In the richest flame with ϕ = 4.5, O atoms are consumed basically via HOPO-involving reactions R7 and R8 that may be determined by a high concentration of HOPO comprising more than 50% of the flame phosphorus. The specific feature of the inhibition chemistry of the rich flame consists of a significant rate of O-atom formation via reaction R9. In the flames with ϕ = 0.7 and 1.5, the net rate of reaction R9 is negligibly low and its graphical presentation is impossible. It may be connected with a very low PO level, which increases in many times in the flame with ϕ = 4.5. Consequently, it reduces the total rate of O-atom consumption via PCS-involving reactions in the rich flames.

Reaction R12 makes a relatively small contribution to the total rate of O consumption in all studied flames, but its contribution still slightly increases with a rise of the equivalence ratio.

The total rate of O consumption via PCS-involving reactions analogous to the hydrogen atoms mainly depends upon the O level and PCS composition in the flames. The concentration of O atoms reaches a maximum value in the flame with ϕ = 1.5 being about 40% less in the lean flame and the order of magnitude being less in the richest flame. We believe that this circumstance mainly determines the highest integrated rate of O consumption at ϕ = 1.5 and the lowest integrated rate of O consumption at ϕ = 4.5 (Figure 5). Certainly, the replacement of $HOPO_2$ by HOPO, which is known to be a more effective inhibitor, with the equivalence ratio rising as well as the PO_2 level variation also influences the shape of the curve in Figure 5.

The fact that the maximum concentration of H atoms is observed at a flame with ϕ = 2.5 while the maximum O-atom concentration is observed at ϕ = 1.5 explains why the curves of integrated rates of production of H and O have minimums at different equivalence ratios. Moreover, the non-coincidence of the minimums in Figure 5 justifies our conclusion that the integrated rate of the atom production is mainly determined by their concentration.

As we have demonstrated earlier,[32] it is incorrect to assume that the inhibition effectiveness is determined only by the rate of removal of active chain carriers from the flame. This assumption contradicts the modeling data shown in Figure 4. If the inhibition effectiveness was determined only by the rate of removal of chain carriers from the flame, it would have a maximum at ϕ = 2 (compare Figures 4 and 5).

According to McLean et al.,[13] burning velocities in syngas/air mixtures (except for the richest mixtures) have the greatest sensitivity to the reaction CO + OH = CO_2 + H. This reaction is the basic pathway for conversion of CO into CO_2.[33] Therefore, it is reasonable to suggest that a change in the net rate of this reaction because of the addition of the inhibitor to the flame should correlate with the inhibition effectiveness (E). To test this suggestion, we calculated integrated net rates of this reaction in flames without additives and in those doped with 0.03% TMP (Table 1). The range of integration covered only the reaction zone of the flame and not the entire flame zone, because the inhibition effectiveness is mainly related to the

dx.doi.org/10.1021/ef301036p | Energy Fuels 2012, 26, 5528−5536

Table 1. Integrated Net Rate of Reaction CO + OH = CO_2 + H in the Pure (I_0) and Doped (I) Flames and a Relative Decrease in the Integrated Net Reaction Rate in the Doped Flames $\Delta I = (I_0 - I)/I_0 \times 100\%$[a]

ϕ	I_0 ($\times 10^4$)	I ($\times 10^4$)	ΔI
0.7	1.604	1.523	5.03
1	2.8764	2.707	5.89
1.5	4.200	3.938	6.24
2	4.726	4.379	7.33
2.5	4.720	4.144	12.21
3	4.328	3.580	17.28
4	2.989	2.101	29.72
4.5	2.409	1.379	42.75

[a]In the mechanism,[12] this reaction is represented by three chemical equations with different kinetic parameters; here, we present the sum of the net rates over all three equations.

radical scavenging in the vicinity of the maximum concentration of chain carriers. Figure 8 shows curves of E and ΔI versus the

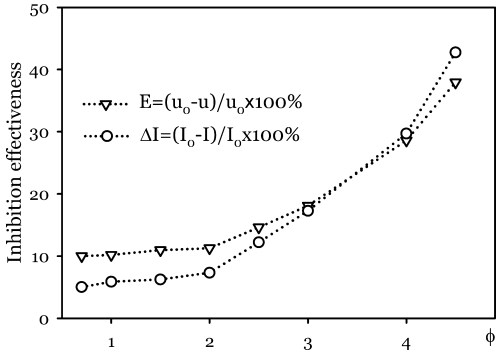

Figure 8. Inhibition effectiveness of atmospheric-pressure syngas/air flames doped with 0.03% TMP, expressed as a decrease in the flame speed because of doping (▽) and the relative decrease in the integrated rate of the reaction CO + OH = CO_2 + H because of doping (○).

equivalence ratio [$\Delta I = (I_0 - I)/I_0 \times 100\%$, where I_0 is the integrated net rate of the reaction in undoped flames and I is the integrated net rate of the reaction in TMP-doped flames]. Both curves reflect the effect of TMP on different flame characteristics: flame speed and the net rate of the basic reaction. There is satisfactory qualitative agreement between the two curves. It is noteworthy that this agreement is observed for syngas flames with a ratio of CO/H_2 = 95:5. Application of this approach for syngas mixtures with a higher hydrogen concentration requires additional study.

It follows from above that the mechanism of inhibition of syngas/air flames by phosphorus compounds involves a decrease in the net rate of the reaction CO + OH. From Figure 9, which shows the spatial variation of the OH concentration in phosphorus-free and TMP-doped flames of various stoichiometries, it can be seen that the decrease in the net reaction rate is due to a reduction in the OH mole fraction with the addition of TMP. Furthermore, the reduction in the OH concentration increases with an increasing equivalence ratio and reaches 40% (the maximum concentration is considered) in the flame with ϕ = 4.5. As a result, there is a reduction in the integral of the net rate of the reaction CO + OH in the doped flame.

We should now explain why the addition of TMP decreases the OH concentration in the flames despite OH formation in reactions involving PCS. It is clear that the reduction in the OH concentration in the inhibited flames, despite OH production in reactions involving the inhibitor, is due to a decrease in the OH production rate in syngas oxidation. The decrease in the rate of OH production in reactions of syngas combustion is much greater than the rate of OH production in reactions involving PCS. The decrease in the OH production rate, in turn, results from a reduction in H and O concentrations in reactions involving TMP and related species. Spatial variations of H and O concentrations in flames without additives and those doped with 0.03% TMP are given in Figure 10. As stated above, the reduction in the OH concentration may be due to a decrease in the net rate of OH production reactions involving H and O atoms. To identify basic reactions, which mainly contribute to a decrease of the OH production rate, we compared the spatial variation of net rates of all OH-producing reactions from the syngas mechanism in clear and TMP-doped flames. The following reactions were shown to play a key role:

$$H + O_2 = O + OH \quad (R13)$$

$$O + H_2 = H + OH \quad (R14)$$

$$HO_2 + H = OH + OH \quad (R15)$$

$$HO_2 + O = O_2 + OH \quad (R16)$$

Figure 11 presents net rate profiles of reactions R13 and R14 in two flames with ϕ = 2.5 and 4.5. We chose these two rich flames because the TMP effect here is more illustrative in comparison to that in stoichiometric and lean flames.

The addition of the inhibitor to the flame with ϕ = 2.5 results in insignificant changes in the net rate of reactions R13 and R14. Reactions R15 and R16, involving HO_2 and proceeding in the low-temperature flame region, make the main contribution to the decrease in the OH concentration. The contribution of reaction R15 is especially substantial because it produces two OH radicals. The addition of TMP to the flame with ϕ = 4.5 substantially reduces the net rate of all of the reactions. However, whereas the maximum net rate of reactions R13 and R14 decreases by a factor of 1.7−1.8, the maximum net rate of reaction R15 decreases by a factor of 3. Reaction R16 does not greatly contribute to the reduction in the OH concentration because its rate is much lower than that of reactions R13−R15.

4. CONCLUSION

Thus, the mechanism of inhibition of syngas/air flames by TMP can be briefly described as follows: Consumption of H and O atoms in catalytic recombination reactions reduces their concentration in the flames. As a result, the net rate of the reactions of OH formation included in the model for syngas oxidation decreases, causing a reduction in the OH concentration in the flames. This, in turn, leads to a decrease in the net rate of the basic reaction of CO oxidation CO + OH = CO_2 + H, which largely controls the flame speed. OH production in reactions involving PCS is a surprising and interesting result, although it does not have a significant influence on the inhibition effectiveness. It should be noted that the proposed scheme is simplified and does not take into account all factors influencing the dependence of the equivalence ratio upon the inhibition effectiveness.

It is just the influence of the inhibitor-related compounds on the H-atom concentration that plays a crucial role in the

dx.doi.org/10.1021/ef301036p | Energy Fuels 2012, 26, 5528−5536

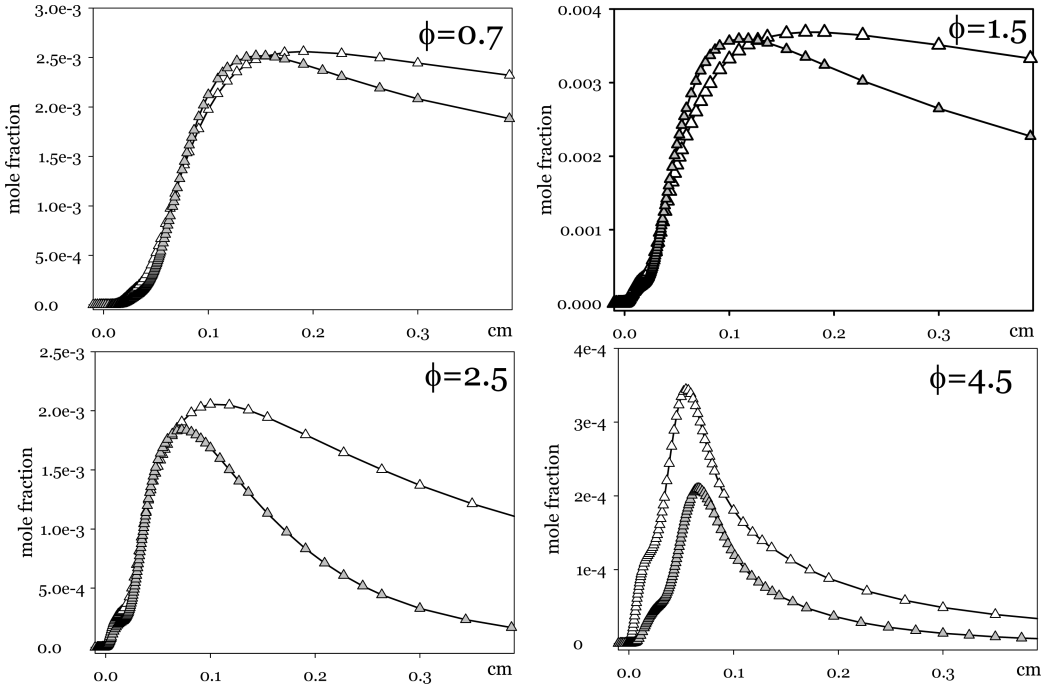

Figure 9. Spatial variation of the OH mole fraction in the undoped (△) and TMP-doped flames (gray ▲).

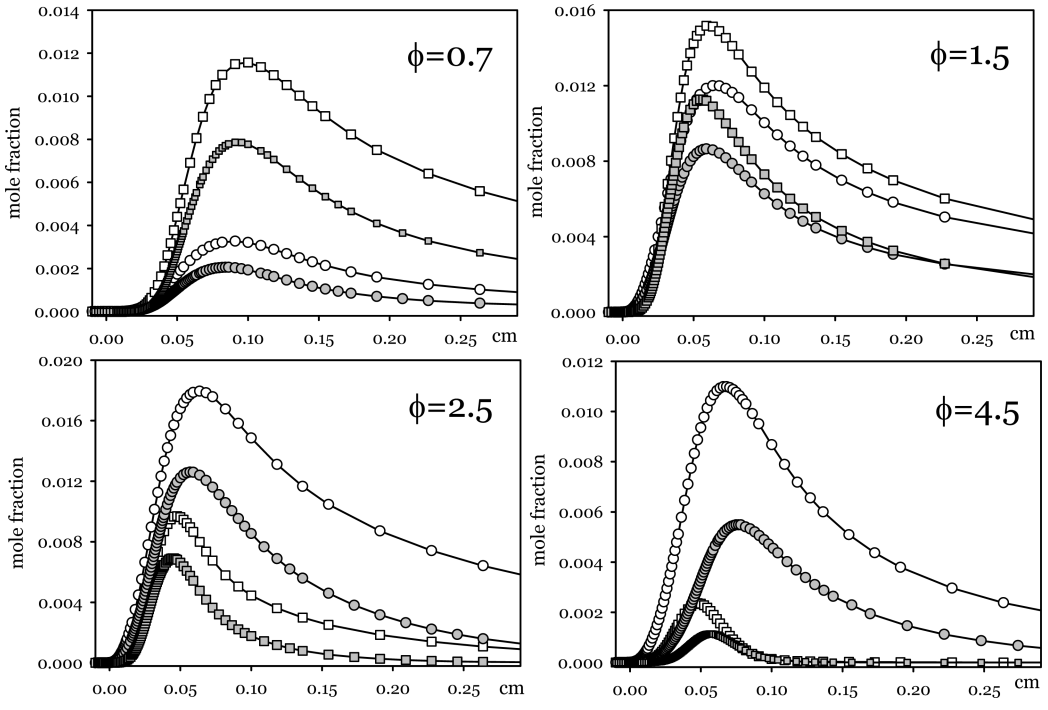

Figure 10. Spatial variation of H (○ and gray ●) and O (□ and gray ■) mole fractions in the undoped (○ and □) and TMP-doped (gray ● and gray ■) flames.

inhibition of syngas/air flames by TMP. The total rate of consumption of H and O atoms via PCS-involving reactions is basically determined by the level of the atoms and PCS composition in the flames rather than the flame temperature.

Despite differences in combustion chemistry between hydrogen and syngas, there is a similarity between their flames in the behavior of the inhibition effectiveness versus the equivalence ratio. In syngas and hydrogen flames,[34] the inhibition effectiveness increases with an increase of the equivalence ratio and reaches a maximum in the richest flames. Moreover, in the case of hydrocarbon flames doped with TMP, the modeling predicts an increase in the effectiveness as ϕ increases from 0.8 to 1.2−1.3.[31] A further increase in the inhibition effectiveness does not occur because of the formation of inactive products of TMP combustion in rich flames. Previously,[26] an increase in the inhibition effectiveness with an increasing ϕ was explained by an increase in the concentration of HOPO, a more active catalyst of chain carrier recombination and, hence, by an increase in the rate of removal of radicals. In the present work, we have demonstrated that the consumption

dx.doi.org/10.1021/ef301036p | Energy Fuels 2012, 26, 5528−5536

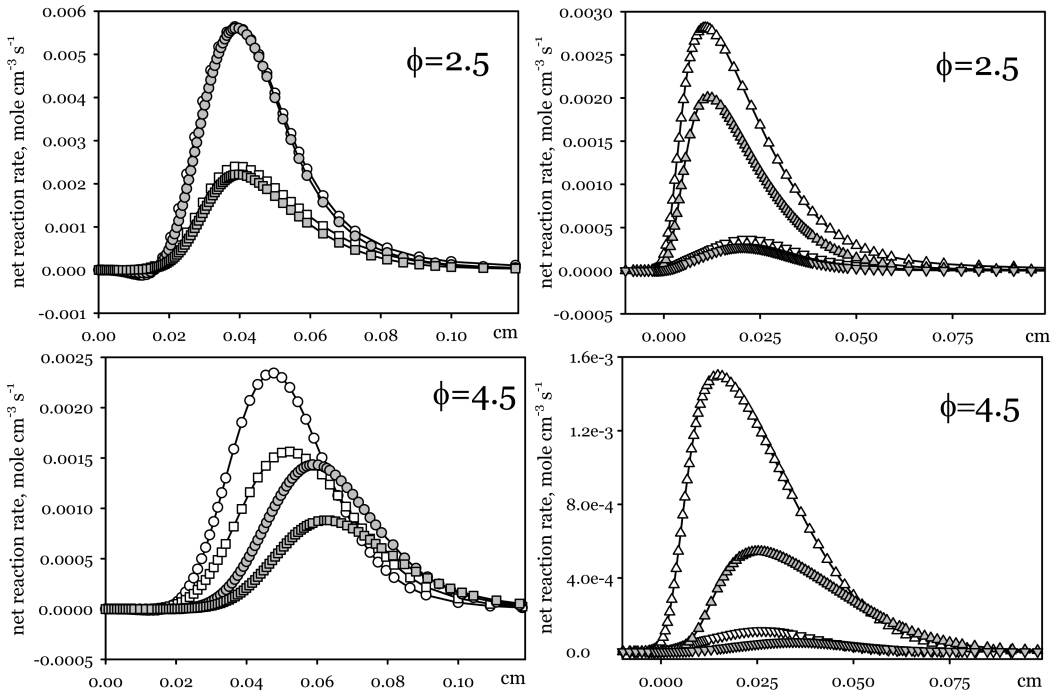

Figure 11. Spatial variation of the net rate of reactions R13 (○ and gray ●), R14 (□ and gray ■), R15 (△ and gray ▲), and R16 (▽ and gray ▼) in atmospheric-pressure syngas/air flames without additive (○, □, △, and ▽) and doped with 0.03% TMP (gray ●, gray ■, gray ▲, and gray ▼).

rate of chain carriers passes through a maximum at $\phi = 2$. This suggests that the high inhibition effectiveness may be related to the relatively low flame temperature near the upper flame propagation limits; e.g., for a syngas/air flame with $\phi = 4.5$, $T_{max} = 1535$ K. At low temperatures, chain branching proceeds at a low rate because of the high activation energy of the reaction H + O_2 = O + OH. At the same time, the inhibition reactions generally have relatively low activation energies and are therefore less sensitive to the temperature.

The mechanism for flame inhibition by TMP[26] generally showed good predictability but does not predict the minimum of the inhibition effectiveness at $\phi = 1.5$. This may be attributed to a shortcoming of the model.[26]

AUTHOR INFORMATION

Corresponding Author

*Telephone: +7 (383) 333-33-46. Fax: +7 (383) 330-73-50. E-mail: vshvarts@kinetics.nsc.ru.

Notes

The authors declare no competing financial interest.

REFERENCES

(1) Scholte, T. G.; Vaags, P. B. *Combust. Flame* **1959**, *3*, 503−510.
(2) Scholte, T. G.; Vaags, P. B. *Combust. Flame* **1959**, *3*, 511−524.
(3) Dixon-Lewis, G.; Williams, D. J. The oxidation of hydrogen and carbon monoxide. In *Comprehensive Chemical Kinetics*; Branford, C. H., Tipper, C. F. H., Eds.; Elsevier: Amsterdam, The Netherlands, 1977; pp 1−248.
(4) Gardiner, W. C., Jr.; Olson, D. B. *Annu. Rev. Phys. Chem.* **1980**, *31*, 377−399.
(5) Westbrook, C. K.; Dryer, F. L. *Prog. Energy Combust. Sci.* **1984**, *10* (1), 1−57.
(6) Yetter, R. A.; Dryer, F. L.; Rabitz, H. *Combust. Sci. Technol.* **1991**, *79*, 97−128.
(7) Kim, T. E. J.; Yetter, R. A.; Dryer, F. L. *Proc. Combust. Inst.* **1994**, *25*, 759−766.
(8) Mueller, M. A.; Kim, T. E. J.; Yetter, R. A.; Dryer, F. L. *Int. J. Chem. Kinet.* **1999**, *31*, 113−125.
(9) Davis, S. G.; Joshi, A. V.; Wang, H.; Egolfopoulos, F. *Proc. Combust. Inst.* **2005**, *30*, 1283−1292.
(10) Saxena, P.; Williams, F. A. *Combust. Flame* **2006**, *145*, 316−323.
(11) Natarajan, J.; Lieuwen, T.; Seitzman, J. *Combust. Flame* **2007**, *151*, 104−119.
(12) Sun, H.; Yang, S. I.; Jomaas, G.; Law, C. K. *Proc. Combust. Inst.* **2007**, *31*, 439−446.
(13) McLean, I. C.; Smith, D. B.; Taylor, S. C. *Proc. Combust. Inst.* **1994**, *25*, 749−757.
(14) Hassan, M. I.; Aung, K. T.; Faeth, G. M. *J. Prop. Power* **1997**, *13* (2), 239−245.
(15) Li, J.; Zhao, Z.; Kazakov, A.; Chaos, M.; Dryer, F. L.; Scire, J. J., Jr. *Int. J. Chem. Kinet.* **2007**, *39*, 109−136.
(16) Wierzba, I.; Kilchyk, V. *Int. J. Hydrogen Energy* **2001**, *26* (6), 639−643.
(17) Safieh, H. Y.; Vandooren, J.; Van Tiggelen, P. J. *Proc. Combust. Inst.* **1982**, *19*, 117−126.
(18) Vandooren, J.; Nelson da Cruz, F.; Van Tiggelen, P. J. *Proc. Combust. Inst.* **1988**, *22*, 1587−1595.
(19) Linteris, G. T. *Combust. Flame* **1996**, *107*, 72−84.
(20) Chang, W. D.; Karra, S. B.; Senkan, S. M. *Combust. Flame* **1987**, *69*, 113−122.
(21) Rumminger, M. D.; Linteris, G. T. *Combust. Flame* **2000**, *4*, 451−464.
(22) Mache, H.; Hebra, A. *Sitzungsber.—Oesterr. Akad. Wiss., Math.-Naturwiss. Kl., Abt. 2a* **1947**, *150*, 157.
(23) Andrews, G. E.; Bradley, D. *Combust. Flame* **1972**, *18*, 133−153.
(24) Linteris, G. T.; Truett, G. T. *Combust. Flame* **1996**, *105* (1−2), 15−27.
(25) Bouvet, N.; Chauveau, C.; Gokalp, I.; Halter, F. *Proc. Combust. Inst.* **2011**, *33*, 913−920.
(26) Jayaweera, T. M.; Melius, C. F.; Pitz, W. J.; Westbrook, C. K.; Korobeinichev, O. P.; Shvartsberg, V. M.; Shmakov, A. G.; Curran, H. *Combust. Flame* **2005**, *140* (1−2), 103−115.
(27) Turanyi, T.; Zsely, I. G.; Frouzakis, C. *KINALC: A CHEMKIN Based Program for Kinetic Analysis*; http://garfield.chem.elte.hu/Combustion/kinalc.htm.

(28) Kee, R. J.; Grcar, J. F.; Smooke, M. D.; Miller, J. A. *A Program for Modeling Steady, Laminar, One-Dimensional Premixed Flames*; Sandia National Laboratories: Albuquerque, NM, 1985; Report SAND85-8240.
(29) Kee, R. J.; Rupley, F. M.; Miller, J. A. Chemkin, I. I. *A Fortran Chemical Kinetics Package for the Analysis of Gas-Phase Chemical Kinetics*; Sandia National Laboratories: Albuquerque, NM, 1989; Report SAND89-8009.
(30) Turanyi, T. *Mechmod Version 1.4: Program for the Transformation of Kinetic Mechanisms*; http://garfield.chem.elte.hu/Combustion/mechmod.htm.
(31) Rybitskaya, I. V.; Shmakov, A. G.; Shvartsberg, V. M.; Korobeinichev, O. P. *Combust., Explos. Shock Waves (Engl. Transl.)* **2008**, *44* (2), 133−140.
(32) Shvartsberg, V. M.; Bolshova, T. A.; Korobeinichev, O. P. *Energy Fuels* **2010**, *24* (3), 1552−1558.
(33) Vagelopoulos, C. M.; Egolfopoulos, F. N. *Proc. Combust. Inst.* **1994**, *25*, 1317−1323.
(34) Korobeinichev, O. P.; Rybitskaya, I. V.; Shmakov, A. G.; Chernov, A. A.; Bolshova, T. A.; Shvartsberg, V. M. *Proc. Combust. Inst.* **2009**, *32*, 2591−2597.